Subterahertz electrodynamics of the graphenelike superconductor CaAlSi

S. Lupi,[1] L. Baldassarre,[1] M. Ortolani,[2] C. Mirri,[1] U. Schade,[2] R. Sopracase,[1] T. Tamegai,[3] R. Fittipaldi,[4] A. Vecchione,[4] and P. Calvani[1]

[1]*CNR-INFM "Coherentia" and Dipartimento di Fisica, Università di Roma La Sapienza, Piazzale A. Moro, 2, 00185 Roma, Italy*

[2]*Berliner Elektronenspeicherring-Gesellschaft für Synchrotronstrahlung mbH, Albert-Einstein Strasse 15, D-12489 Berlin, Germany*

[3]*Department of Applied Physics, The University of Tokyo, 7-3-1 Hongo, Bunkyo-ku, Tokyo 113-8656, Japan*

[4]*CNR-INFM Laboratorio Regionale Supermat and Dipartimento di Fisica "E. R. Caianiello," Università degli Studi di Salerno, Via S. Allende, 84081 Baronissi Salerno, Italy*

(Received 14 December 2007; published 25 February 2008)

We report an optical study of CaAlSi, a superconductor which displays both the crystal structure of MgB_2 and the electronic band structure of intercalated graphites. The reflectivity of a CaAlSi single crystal was measured down to subterahertz frequencies and to 3.3 K, with the use of coherent synchrotron radiation. A single superconducting gap in the hexagonal planes and two gaps along the *c* axis were found and measured consistently with the structure of the CaAlSi Fermi surface. The normal-state optical conductivity is also anisotropic: in the *ab* plane, the plasma frequency is larger by more than a factor of 2 than along the *c* axis. An analysis of the *ab*-plane spectral weight in comparison with the corresponding quantity in a cuprate such as $La_{2-x}Sr_xCuO_4$ shows that in CaAlSi the correlation effects are negligible.

DOI: 10.1103/PhysRevB.77.054510 PACS number(s): 74.25.Gz, 74.78.Db, 78.30.−j

I. INTRODUCTION

In the last few years, much interest has been devoted to the superconducting (SC) properties of graphenelike compounds such as MgB_2, up to now, the conventional Bardeen-Cooper-Schrieffer (BCS) superconductor with the highest T_c, and the intercalated graphites CaC_6 and YbC_6. All these compounds have *ab* planes with hexagonal symmetry, although differently stacked along the *c* axis. This reflects into a *k* space with electronic σ, π, and interlayer (IL) bands which are differently filled in different members of the family.[1] MgB_2 is hole doped, with the Fermi level crossing a two-dimensional σ band and a three-dimensional (3D) π band.[2] As a result, it presents two distinct SC gaps. In turn, CaAlSi (Ref. 3) is electron doped like CaC_6: the σ bands are completely filled and the bottom of the IL band crosses the Fermi level together with the π bands,[4–6] again as in intercalated graphites. The order parameter of CaAlSi is reported to have an *s*-anisotropic symmetry,[7] but it is not clear if there are one or two gaps. The available experimental data are not conclusive in this respect. While angle resolved photoemission spectroscopy (ARPES)[8] distinguished in CaAlSi one isotropic gap of about 1.2 meV=4.2 k_BT_c, muon spin rotation (μSR) data[9] suggested a highly anisotropic gap or possibly two distinct gaps as in MgB_2. Penetration depth measurements[7] are interpreted in terms of a single, moderately anisotropic *s*-wave gap. Whether the gap is single or not is an important issue, as two coexisting order parameters may lead to an enhancement of T_c.[10,11] Recently, μSR experiments have reported the existence of a second gap in the *ab* planes of high-T_c superconductors.[12]

Infrared spectroscopy allows the direct measurement of the optical gap of a superconductor along different crystal axes, with an energy resolution higher than that in ARPES. This can be done also in low-T_c materials[13] with the needed signal-to-noise ratio, with a conventional interferometer and a liquid-He bolometer, provided that the source is coherent synchrotron radiation (CSR).[14] Here, we apply this technique to study the electrodynamics of CaAlSi. As shown above, it may be considered as a model system for the graphenelike superconductors. Moreover, unlike other members of the family, crystals can be grown with all the three dimensions large enough for optical observations in the millimeter-wavelength domain.

II. EXPERIMENT AND RESULTS

The sample was a single crystal of $2\times4.5\times3$ mm^3. It was grown by the floating-zone method and characterized, as described in Ref. 15. X-ray diffraction showed an admixture of the fivefold and sixfold superstructures reported[16] for CaAlSi. The cell parameter *c* was 0.4388 nm. Both surfaces were accurately polished with a 0.5 μm thick diamond powder. After polishing, their alignment with respect to the crystal axes was controlled once again by electron backscatter diffraction in different points. The sample magnetic moment $M(T)$ was also measured after the polishing and reported in the inset of Fig. 1. It shows the SC transition with an onset at 6.7 K. This temperature, where the resistivity is already equal to zero, is the best estimate of T_c as $M(T)$ is a bulk quantity like the infrared conductivity.

By assuming that CaAlSi is a conventional, weak-coupling superconductor, we may expect a superconducting gap $2\Delta\simeq3.5k_BT_c/hc\simeq16$ cm^{-1} $\simeq$0.5 THz. In order to measure the reflectivity within a few parts per thousand at subterahertz frequencies, we illuminated the sample with the CSR extracted from the electron storage ring BESSY, working in the so-called low-α mode[14] at a beam current $i\sim20$ mA. CSR is free of thermal noise and, in the subterahertz range, is more brilliant than any other broadband radiation source by at least 3 orders of magnitude.[14] The sample was mounted on a copper cone, which scattered away the radiation not impinging onto the sample. This made the zone around the sample optically black. We also checked that any

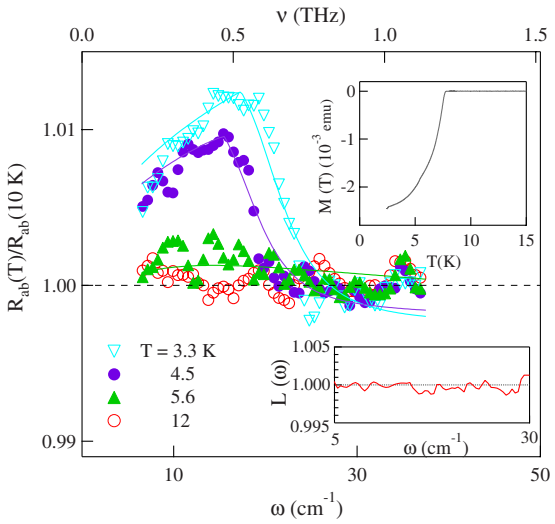

FIG. 1. (Color online) Ratio between the subterahertz reflectivity of the *ab* planes below T_c and in the normal phase at 10 K. The lines are fits based on a BCS reflectivity below T_c and on a Hagen-Rubens model at 10 K. The upper inset shows the magnetic moment measured by cooling the sample in a field of 10 Oe, showing the superconducting transition at T_c=6.7 K. The lower inset shows a check on data reproducibility, performed by dividing two subsequent spectra of 256 scans. The error is on the order of 0.1%.

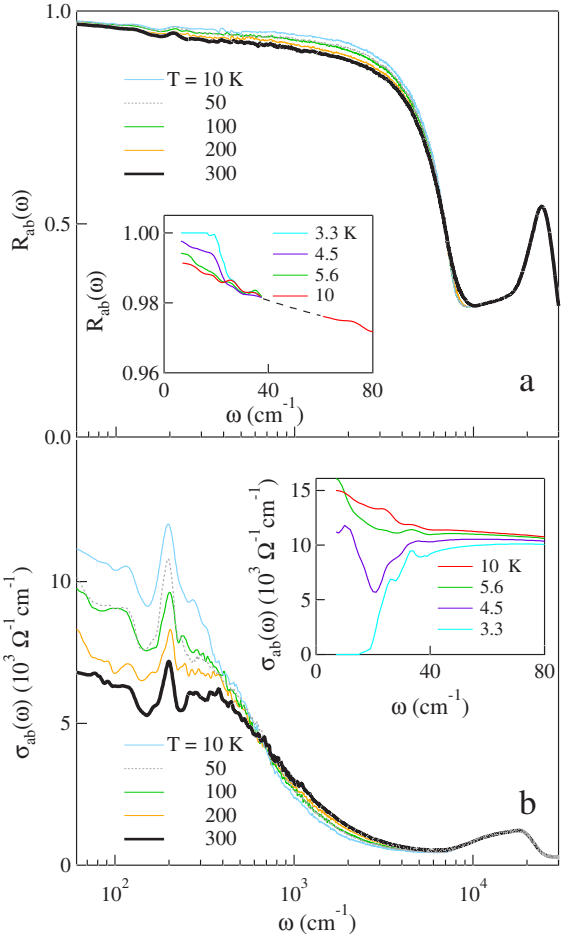

FIG. 2. (Color online) Optical response of the hexagonal planes of CaAlSi. (a) Absolute reflectivity at different temperatures; the inset shows the reflectivity in the terahertz range above and below T_c, as reconstructed from the ratios in Fig. 1. (b) Optical conductivity from the reflectivity in (a); the inset shows the conductivity of the hexagonal planes in the subterahertz range.

residual effect of diffraction at the longest wavelengths could be ruled out by placing mirrors of decreasing diameter in front of the sample. We verified that the signal-to-noise ratio remained unaltered down to a diameter of 2 mm and to a frequency of 5 cm^{-1}. Moreover, the reproducibility between two subsequent spectra of 256 scans was on the order of 0.1%, as shown in the lower inset of Fig. 1.

After those tests, we measured at different temperatures the radiation intensity reflected in the subterahertz range by the sample, $I_R(T)$, as described in Ref. 13. The changes in the ring current were taken into account by measuring, with an automatic procedure, the intensity transmitted through the interferometer before any measurement of $I_R(T)$. The very high reflectivity of the sample and its thickness also excluded any possibility of multiple reflections. By using a commercial interferometer and a bolometer working at 1.6 K, we thus reduced the error in the superconducting gap region on the reflected intensity $\Delta I_R/I_R$ to ~0.1%. We then determined the ratio $I_R(T)/I_R(10\ K)$, which for $T<T_c$ and in the present experimental conditions coincides with the reflectivity ratio $R(T)/R(10\ K)$. The function $R_s/R_n(\omega)$ is expected to exhibit a peak[17] at $\omega=2\Delta$.

A. Optical response of the *ab* plane

The ratio $R(T)/R(10\ K)$ is reported in Fig. 1 for the radiation polarized in the hexagonal sheets at T, both below and above T_c. As in the normal state $R(10\ K)\simeq 0.99$ at low ω [see Fig. 2(a)], the total variation of $R_{ab}(T)/R_{ab}(10\ K)$ between T=3.3 and 8 K is just slightly more than 1%. In Fig. 1, the curves at $T<T_c$ exhibit the expected peak at $2\Delta_{ab}(T)$, while for $T>T_c$ (12 K), the above ratio is equal to 1 at any ω within the noise. At 3.3 K, the peak frequency is about 17 cm^{-1}, which gives $2hc\Delta/k_BT_c\simeq 3.8$. It is then reasonable to use the BCS theory to fit the data. We modeled the optical conductivity $\sigma(\omega)$, for the hexagonal planes in the normal state, by a conventional Drude model with the plasma frequency ω_{ab}^0 and the scattering rate Γ_{ab} determined by a fit to the normal state (T=10 K) optical conductivity (see below). In the SC state, we used the Mattis-Bardeen model[18] with a fixed T_c=6.7 K and Δ_{ab} as a free parameter. The curves $R(\omega,T)/R(\omega,10\ K)$ calculated in this way are also reported in Fig. 1. The fit is good at the three temperatures and provides $2\Delta_{ab}$=15 and 17.5 cm^{-1} at 4.5 and 3.3 K, respectively. This leads to an extrapolated value[18] $2\Delta_{ab}(0)=19.0\pm 1.5\ cm^{-1}$, or $2hc\Delta_{ab}(0)/k_BT_c=4.1\pm 0.4$, a value which confirms—with the higher resolution provided by infrared spectroscopy—a previous determination by ARPES.[8] The gap has also been recently measured by tunneling spectroscopy[19] in CaAlSi with three different superstructures. In the fivefold and sixfold superstructures, the authors find $hc\Delta(0)$=0.9 and 1.3 meV, respectively. These values can be compared with the present determination of 1.2 meV

in a sample which shows an admixture of the above two superlattices. These results suggest that CaAlSi is a BCS superconductor with a moderately strong coupling. On the basis of our fits, a single gap well describes the superconducting transition in the hexagonal planes.

Once we determined the above reflectivity ratios in the subterahertz region, we measured the absolute reflectivity $R_{ab}(T)$ at any T from 60 to 12 000 cm^{-1}, where R depends on T, and up to 25 000 cm^{-1} at 300 K. Below 18 000 cm^{-1}, we used a Michelson interferometer, and between 18 000 and 25 000 cm^{-1}, a grating monochromator equipped with a charge coupled device detector. We took as reference the crystal itself, gold coated by *in situ* evaporation below 12 000 cm^{-1} and silver coated above this frequency. The results are shown in Fig. 2(a). We assumed $R(3.3\ K)=1$ for $\omega \leqslant 2\Delta$ and we scaled[13] the subterahertz $R_{ab}(T)$ at any T according to the ratios in Fig. 1. Between 60 and 35 cm^{-1}, we interpolated the data with the Hagen-Rubens model. We thus obtained at any ω and T the absolute reflectivity of the *ab* planes, which was then used to extract the real part of the optical conductivity $\sigma(\omega)$ by standard Kramers-Kronig transformations. At a first inspection of Fig. 2(a), the plasma edge in the $R(\omega)$ of CaAlSi falls at ~8000 cm^{-1} to be compared with[20] ~17 000 cm^{-1} in MgB_2.

The real part of the optical conductivity $\sigma_{ab}(\omega)$ of the hexagonal planes is shown in Fig. 2(b). For $T<T_c$, it decreases in the subterahertz range, showing the opening of the superconducting gap. As reported below, here $\Gamma_{ab}(T_c) \simeq 500\ cm^{-1} \gg \Delta_{ab}(0)$ (dirty limit). Therefore, according to the Ferrell-Glover-Tinkham (FGT) sum rule, the spectral weight W_s condensed at $\omega=0$ below T_c is[18]

$$W_s(T) = \int_{0+}^{6\Delta} [\sigma_n(\omega,T) - \sigma_s(\omega,T)]d\omega, \tag{1}$$

where σ is expressed in cm^{-1} and it is assumed [see the inset of Fig. 2(b)] that W_s saturates above $6\Delta \simeq 60\ cm^{-1}$. This is therefore the range of validity of the FGT sum rule. Equation (1) can be used to evaluate the field penetration depth λ. From $\lambda(T)=1/[8W_s(T)]^{1/2}$, one extracts λ_{ab} (3.3 K) $=2250\pm200$ nm. As in the dirty limit[18] $\lambda \sim \lambda^L(\Gamma/\Delta)^{1/2}$, where λ^L is the London penetration depth, one obtains λ^L_{ab} (3.3 K) $=300\pm30$ nm, in excellent agreement with λ^L_{ab} (3.3 K) $=330$ nm extracted from high-precision susceptibility measurements.[7]

In the normal state, $\sigma_{ab}(\omega)$ shows a standard Drude behavior below about 1 eV, with a plasma frequency ω^0_{ab} $=20\,000\ cm^{-1}$ nearly independent of temperature. The same value comes out from density functional theory calculations, after renormalization for the electron-phonon coupling.[21] This value should be compared with $\omega^0_{ab} \simeq 45\,000\ cm^{-1}$ in[20] MgB_2 and a scattering rate $\Gamma_{ab}=480\ cm^{-1}$ at 10 K (850 cm^{-1} at 300 K). Figure 2(b) also shows an unshielded phonon peak at 195 cm^{-1}, independent of T, which can be identified with the E_{1u} in-plane stretching mode predicted between[4–6] 183 and 194 cm^{-1}. The broad electronic band between 10 000 and 20 000 cm^{-1} can be assigned to the transitions between the antibonding π band and the $3d_{z^2-r^2}$ band of the local density approximation calculations.[5]

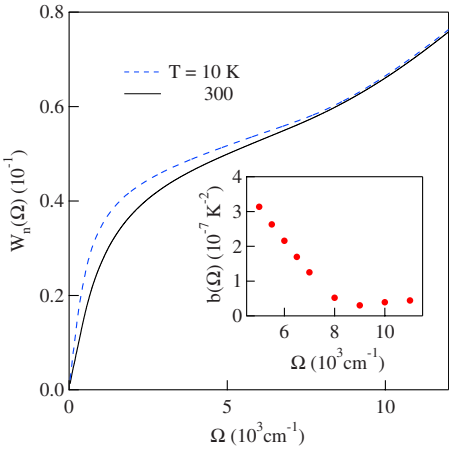

FIG. 3. (Color online) Spectral weight in the *ab* plane of CaAlSi vs the cutoff frequency Ω at two temperatures in the normal phase. The inset shows the normalized thermal response of the carriers as a function of Ω (see text).

The *ab*-plane spectral weight of CaAlSi can be calculated also in the normal phase, at different temperatures, through

$$W_n(\Omega,T) = \int_0^{\Omega} \sigma_n(\omega,T)d\omega. \tag{2}$$

This quantity is plotted as a function of Ω at two temperatures (300 and 10 K) in Fig. 3. As one can see, the two curves cannot be distinguished any more above 8000 cm^{-1}, a frequency corresponding to the plasma edge in the reflectivity of Fig. 2. This shows that a restricted *f*-sum rule is verified for CaAlSi within the Drude absorption of the free carriers. Such behavior is similar to that observed in a conventional metal such as gold.[22] On the contrary, in the *ab* plane of high-T_c cuprates, the *f*-sum rule is not fulfilled unless the cutoff frequency Ω is much larger than the plasma edge. This anomaly has been attributed to the effect of strong correlations, which mix the high- and low-energy scales in the optical response of the carriers.[23] Both in conventional metals and in a cuprate such as $La_{2-x}Sr_xCuO_4$, moreover, the spectral weight depends on temperature as

$$W_n(\Omega,T) = W_0[1 - b(\Omega)T^2]. \tag{3}$$

Therein, the frequency-dependent coefficient b describes the "thermal response" of the carriers, while W_0—in a one-band tight binding model—is proportional to their hopping rate t_0. In correlated materials, unlike in a conventional Fermi liquid, $b(\Omega)$ is appreciably different from zero well beyond the plasma edge ω_p.[22] For example, in $La_{2-x}Sr_xCuO_4$ with $x=0.12$, $b(\omega_p)=2.5\times10^{-7}\ K^{-2}$. The inset of Fig. 3 shows that in CaAlSi, $b(\Omega)$ is smaller ($5\times10^{-8}\ K^{-2}$) and more similar to that of gold [$b(\omega_p)=2\times10^{-8}\ K^{-2}$]. Therefore, the present analysis of the T dependence of the spectral weight provides a clear confirmation that in CaAlSi, the effect of electron correlations is negligible.

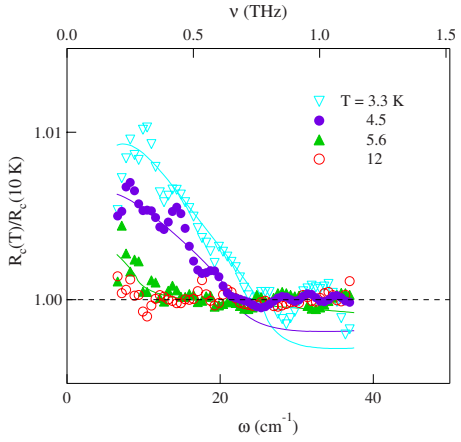

FIG. 4. (Color online) Ratio between the subterahertz reflectivity of the c axis below T_c and that in the normal phase at 10 K. The lines are fits to a two-gap model, see text.

B. Optical response of the c axis

Let us now consider the optical response of CaAlSi along the c axis. Figure 4 shows the ratio $R_c(T)/R_c(10\ \mathrm{K})$, as measured with the radiation polarized along the c direction. Here also, the total variation of the reflectivity between 10 and 3.3 K is barely 1%, due to the extremely high reflectivity in the normal phase [see Fig. 5(a)]. A peak appears below T_c, as in Fig. 1, but with a different shape. Such a shape suggests that either only a fraction of the carriers contribute to the optical conductivity of the SC phase or there are two distinct gaps. The former case is observed, for example, in high-T_c cuprates, where the order parameter has nodes in the k space due to its d-wave symmetry, but this should be excluded in CaAlSi.[21] The second situation is that of MgB_2, where a two-gap model well accounts for the reflectivity data below T_c.[24] In CaAlSi, the two gaps should come out from different regions of the Fermi surface, which is topologically disconnected along the k_z direction. By applying the same model to the $R_c(T<T_c)/R_c(10\ \mathrm{K})$ of Fig. 4, one finds the fitting curves shown in the figure as solid lines, which well fit the data. The resulting values for the two gaps are $2\Delta_{c,1}=22\ \mathrm{cm}^{-1}$ at 4.5 K, $26\ \mathrm{cm}^{-1}$ at 3.3 K, and $28\ \mathrm{cm}^{-1}$ extrapolated to 0 K; in turn, $2\Delta_{c,2}=2$, 6, and 8 cm^{-1} at 4.5, 3.3, and 0 K, respectively. It is reasonable to associate the two gaps to the bands which cross the Fermi level. According to the fit, the corresponding plasma frequencies are $\omega^0_{c,1}=5500\ \mathrm{cm}^{-1}$ and $\omega^0_{c,2}=7100\ \mathrm{cm}^{-1}$. Unlike in MgB_2, however, in CaAlSi, both those bands have a 3D character and therefore one should expect two gaps also in the ab plane. However, in that plane, the Fermi surface is substantially connected topologically[5] and a one-gap model is expected to well fit the observations, as indeed shown in Fig. 1. One may also remark that $\Delta_{ab}<\Delta_{c,1}$. Using here a higher energy resolution than in ARPES, we have thus found a moderate anisotropy of the SC state which reflects the symmetry of the electron-phonon coupling[4,5] and may reconcile the ARPES observations with the penetration depth results of Ref. 7.

The absolute $R_c(T)$ was then determined for the c axis as for the ab plane, except for the need to interpolate data taken with different sources. The resulting curves are shown in Fig. 5(a), with the subterahertz range enlarged in the inset. The resulting conductivity $\sigma_c(\omega)$ is reported in Fig. 5(b). At high energies, it exhibits shallow maxima at 4000, 9000, and 12 000 cm^{-1} which can be ascribed to the folding of the Brillouin zone resulting from the superstructures found by x rays along the c axis of our crystal. The Drude term along the c axis has an $\omega^0_c=9000\ \mathrm{cm}^{-1}$ $[(\omega^0_c)^2=(\omega^0_{c,1})^2+(\omega^0_{c,2})^2]$ and Γ_c of 180 cm^{-1} at 10 K and 235 cm^{-1} at 300 K. The phonon peak at 205 cm^{-1} can be assigned to the A_{2u} out-of-plane stretching mode, expected between[4–6] 212 and 222 cm^{-1}. For $T<T_c$, $\sigma_c(\omega)$ decreases in the subterahertz range, showing the opening of the superconducting gap. As for the ab plane, we estimated the spectral weight condensed below T_c at $\omega=0$ by Eq. (1). This gives λ_c (3.3 K) $=4000\pm400$ nm and λ^L_c (3.3 K) $=900\pm100$ nm. The value reported in Ref. 7 for λ^L_c at the same temperature is 725 nm.

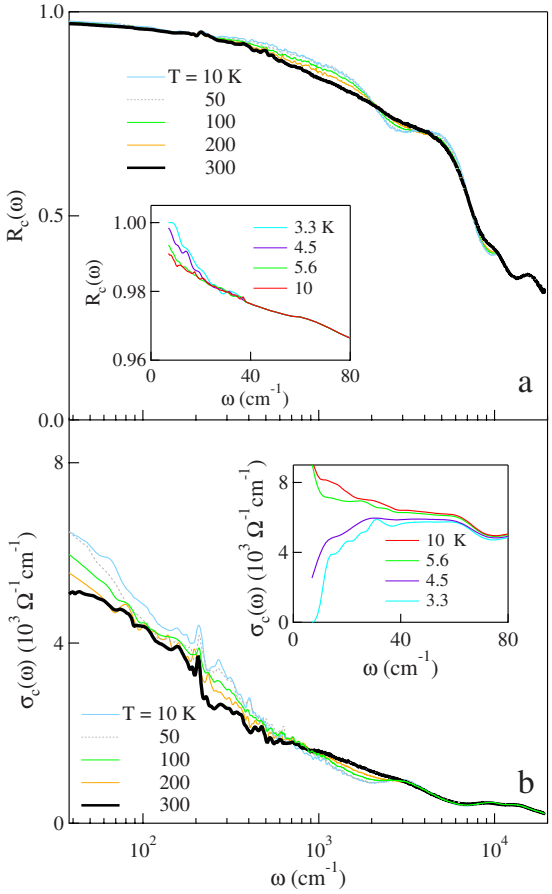

FIG. 5. (Color online) Optical response of the c axis of CaAlSi. (a) Absolute reflectivity at different temperatures; the inset shows the reflectivity in the terahertz range above and below T_c, as reconstructed from the ratios in Fig. 4. (b) Optical conductivity obtained from the reflectivity in (a); the inset shows the conductivity of the c axis in the subterahertz range.

III. CONCLUSION

In conclusion, we have studied experimentally the electrodynamics of the superconductor CaAlSi from the subtera-

hertz region to the visible range. The use of coherent synchrotron radiation has allowed us to measure the superconducting gap 2Δ both in the hexagonal planes and along the c axis. In both cases, we find $\Gamma(T_c) \gg \Delta(0)$ and, as expected for a noncorrelated system in the dirty limit, the FGT sum rule is fulfilled within $\sim 6\Delta$. In the planes, we obtain good fits by a single gap value, while along c, one needs to introduce two gaps. This anisotropy is consistent with the calculated Fermi surface, which is connected in the k_x, k_y planes, disconnected along the k_z direction. All gap values are consistent with the BCS superconductivity in moderately strong coupling, but $2\Delta_{ab}$ is slightly smaller than the largest $2\Delta_c$. This reflects also in the London penetration depth, with $\lambda_c^L \simeq 3\lambda_{ab}^L$. This moderate anisotropy in the basic parameters of the SC state may partially explain, and possibly reconcile, the contrasting results reported in the literature of CaAlSi by different techniques.

In the normal phase of CaAlSi, the Drude parameters ω_0 and Γ display an anisotropy not observed in MgB_2, being both much larger in the planes than along the c axis. This suggests that the carriers propagating along c have a larger effective mass but longer free paths. An IR-active phonon is also observed, at a frequency very close to that calculated in the literature. Finally, we have determined the temperature dependence of the spectral weight in the ab plane of CaAlSi and compared it with that, reported in a previous paper, of the ab plane of $La_{2-x}Sr_xCuO_4$. We have shown that they are much different from each other, with the former one much closer to that of a conventional metal such as gold. This confirms that correlation effects do not play a role in the optical conductivity of CaAlSi.

ACKNOWLEDGMENT

We wish to thank Danilo Zola for performing the magnetization measurements reported in the inset of Fig. 1.

[1] L. Boeri, G. B. Bachelet, M. Giantomassi, and O. K. Andersen, Phys. Rev. B **76**, 064510 (2007).
[2] J. Nagamatsu, N. Nagakawa, T. Muranaka, Y. Zenitani, and J. Akimitsu, Nature (London) **410**, 63 (2001).
[3] M. Imai, K. Nishida, T. Kimura, and K. Abe, Appl. Phys. Lett. **80**, 1019 (2002).
[4] I. I. Mazin and D. A. Papaconstantopoulos, Phys. Rev. B **69**, 180512(R) (2004).
[5] M. Giantomassi, L. Boeri, and G. B. Bachelet, Phys. Rev. B **72**, 224512 (2005).
[6] G. Q. Huang, L. F. Chen, M. Liu, and D. Y. Xing, Phys. Rev. B **69**, 064509 (2004).
[7] R. Prozorov, T. A. Olheiser, R. W. Giannetta, K. Uozato, and T. Tamegai, Phys. Rev. B **73**, 184523 (2006).
[8] S. Tsuda, T. Yokoya, S. Shin, M. Imai, and I. Hase, Phys. Rev. B **69**, 100506(R) (2004).
[9] S. Kuroiwa, H. Takagiwa, M. Yamazawa, J. Akimitsu, K. Ohishi, A. Koda, W. Higemoto, and R. Kadono, J. Phys. Soc. Jpn. **73**, 2631 (2004).
[10] H. Suhl, B. T. Matthias, and L. R. Walker, Phys. Rev. Lett. **3**, 552 (1959).
[11] S. Tsuda, T. Yokoya, T. Kiss, T. Shimojima, S. Shin, T. Togashi, S. Watanabe, C. Zhang, C. T. Chen, S. Lee, H. Uchiyama, S. Tajima, N. Nakai, and K. Machida, Phys. Rev. B **72**, 064527 (2005).
[12] R. Khasanov, A. Shengelaya, A. Maisuradze, F. La Mattina, A. Bussmann-Holder, H. Keller, and K. A. Müller, Phys. Rev. Lett. **98**, 057007 (2007).
[13] M. Ortolani, S. Lupi, L. Baldassarre, U. Schade, P. Calvani, Y. Takano, M. Nagao, T. Takenouchi, and H. Kawarada, Phys. Rev. Lett. **97**, 097002 (2006).
[14] M. Abo-Bakr, J. Feikes, K. Holldack, P. Kuske, W. B. Peatman, U. Schade, G. Wüstefeld, and H.-W. Hübers, Phys. Rev. Lett. **90**, 094801 (2003).
[15] A. K. Ghosh, M. Tokunaga, and T. Tamegai, Phys. Rev. B **68**, 054507 (2003).
[16] H. Sagayama, Y. Wakabayashi, H. Sawa, T. Kamiyama, A. Hoshikawa, S. Harjo, K. Uozato, A. K. Ghosh, M. Tokunaga, and T. Tamegai, J. Phys. Soc. Jpn. **75**, 043713 (2006).
[17] D. N. Basov, S. V. Dordevic, E. J. Singley, W. J. Padilla, K. Burch, J. E. Elenewski, L. H. Greene, J. Morris, and R. Schickling, Rev. Sci. Instrum. **74**, 4703 (2003).
[18] M. Dressel and G. Grüner, *Electrodynamics of Solids* (Cambridge University Press, Cambridge, 2002).
[19] S. Kuroiwa, T. Takasaki, T. Ekino, and J. Akimitsu, Phys. Rev. B **76**, 104508 (2007).
[20] V. Guritanu, A. B. Kuzmenko, D. Van der Marel, S. M. Kazakov, N. D. Zhigadlo, and J. Karpinski, Phys. Rev. B **73**, 104509 (2006).
[21] L. Boeri and I. Mazin (private communication).
[22] M. Ortolani, P. Calvani, and S. Lupi, Phys. Rev. Lett. **94**, 067002 (2005).
[23] A. Toschi, M. Capone, M. Ortolani, P. Calvani, S. Lupi, and C. Castellani, Phys. Rev. Lett. **95**, 097002 (2005).
[24] M. Ortolani, D. Di Castro, P. Postorino, I. Pallecchi, M. Monni, M. Putti, and P. Dore, Phys. Rev. B **71**, 172508 (2005).